nature methods

BRIEF COMMUNICATION

https://doi.org/10.1038/s41592-018-0168-y

FLIRT: fast local infrared thermogenetics for subcellular control of protein function

Sophia M. Hirsch[1,6], Sriramkumar Sundaramoorthy[2,5,6], Tim Davies[2], Yelena Zhuravlev[1], Jennifer C. Waters[3], Mimi Shirasu-Hiza[1], Julien Dumont[4] and Julie C. Canman[2*]

FLIRT (fast local infrared thermogenetics) is a microscopy-based technology to locally and reversibly manipulate protein function while simultaneously monitoring the effects in vivo. FLIRT locally inactivates fast-acting temperature-sensitive mutant proteins. We demonstrate that FLIRT can control temperature-sensitive proteins required for cell division, Delta–Notch cell fate signaling, and germline structure in *Caenorhabditis elegans* with cell-specific and even subcellular precision.

Molecular control of transient cellular processes such as cell division involves precise spatiotemporal regulation. Fast-acting (≤20 s) temperature-sensitive mutants enable studies of temporally regulated protein function by upshifting cells from permissive to restrictive temperature to conditionally inactivate protein function during the cellular process of interest (Fig. 1a). Current techniques to inactivate fast-acting temperature-sensitive mutants rely on changing the temperature of the whole cell or organism using temperature-controlled stages or specimen holders[1–6]. Although these techniques have high temporal resolution, they are unable to perturb protein function with spatial resolution.

To harness the power of fast-acting temperature-sensitive mutants for high-resolution spatiotemporal studies, we took inspiration from a technique used to locally induce ectopic gene expression[7] and developed FLIRT, which uses infrared light to rapidly and locally control temperature-sensitive mutant protein function. In brief, infrared laser light focused on a distinct subcellular structure or specific cell within an organism locally heat-inactivates temperature-sensitive proteins at precise moments during a cellular behavior, and the effects can be monitored in vivo (Fig. 1a). Here we describe the FLIRT system, validate its ability to alter local temperature in vivo, and demonstrate its precision and resolution in altering temperature-sensitive mutant protein function at cellular and subcellular levels in *C. elegans*.

The FLIRT system is built on an inverted spinning disk confocal microscope equipped with a multimode 1,470-nm-wavelength laser (Supplementary Fig. 1a). We selected 1,470 nm because of the high absorption of water and low cellular toxicity in that spectral region[7]. We control the region targeted for infrared irradiation with a wheel containing different mask shapes and sizes; the infrared mask is then projected onto the specimen plane. We focus the infrared laser at the beginning of each imaging session using photon-upconverting nanoparticles (UCPs) (Supplementary Fig. 1b), which are excited by infrared light but emit visible light[8], allowing precise focus of the laser-targeted region onto the specimen plane[8]. A microfluidic temperature-control system maintains specimen temperature and functions as a heat sink.

To measure and calibrate the temperature change induced by FLIRT, we used two circular masks (16-µm and 27-µm diameter, respectively; Supplementary Fig. 1b) and two independent assays. First, we used a thermochromatic dye that undergoes a temperature-dependent color change from opaque (black) to transparent at 15 °C, altering light transmittance through a glass coverslip painted with this dye (Supplementary Fig. 2). Second, we used an mCherry-based bioassay in *C. elegans* embryos expressing mCherry::HistoneH2B, based on previous work showing that the fluorescence intensity of mCherry emission decreases as sample temperature increases (Supplementary Fig. 3)[9]. We generated calibration curves of the temperature-dependent change in light transmission (thermochromatic dye) or fluorescence intensity (mCherry) across a range of temperatures using the microfluidic temperature control system and compared this to the change in intensity observed with increasing infrared laser power (Supplementary Figs. 2 and 3). Both assays gave similar results. We determined that 0.9 and 1.0 mW of infrared laser power shifted the sample temperature within the targeted area by 1 °C in vivo when we used 16- and 27-µm-diameter circular masks, respectively (Supplementary Fig. 3), and confirmed the expected effects in vivo using whole-cell FLIRT at varying laser powers in temperature-sensitive mutant embryos (Supplementary Note 1).

To test whether FLIRT can inhibit temperature-sensitive (ts) mutant proteins in a cell-specific manner without affecting non-targeted cells, we used a 16-µm-diameter mask to specifically target the division plane in either the anterior cell (AB) or the posterior cell (P1) of control or *myosin-II(ts)* (*nmy-2(ne3409ts)*) embryos at the two-cell stage. Myosin-II is an actin motor protein required for constriction of the actomyosin contractile ring during cytokinesis[10–12]. In *myosin-II(ts)* embryos upshifted to 26 °C, cytokinesis fails in both AB and P1 cells (Supplementary Note 2). In FLIRT-targeted *myosin-II(ts)* embryos, division failed only in the targeted cell but was completed in the other cell (Fig. 1c, Supplementary Fig. 4a, and Supplementary Video 1). When we turned off the infrared laser at approximately 4 min after anaphase onset, both AB and P1 cells divided, indicating that FLIRT-mediated protein inhibition is rapidly reversible (Supplementary Fig. 4b and Supplementary Video 2). In control non-temperature-sensitive mutant embryos, neither cell failed in division, even when targeted with FLIRT throughout contractile ring constriction (Fig. 1c, Supplementary Fig. 4a, and Supplementary Video 1). Thus, FLIRT specifically and reversibly inactivates temperature-sensitive proteins only in the targeted cell of a two-cell embryo.

[1]Department of Genetics and Development, Columbia University Medical Center, New York, NY, USA. [2]Department of Pathology and Cell Biology, Columbia University Medical Center, New York, NY, USA. [3]Department of Cell Biology, Harvard Medical School, Boston, MA, USA. [4]Institut Jacques Monod, CNRS, UMR 7592, Université Paris Diderot, Sorbonne Paris Cité, Paris, France. [5]Present address: VelociGene Division, Regeneron Pharmaceuticals, Tarrytown, NY, USA. [6]These authors contributed equally: Sophia M. Hirsch, Sriramkumar Sundaramoorthy. *e-mail: jcc2210@cumc.columbia.edu

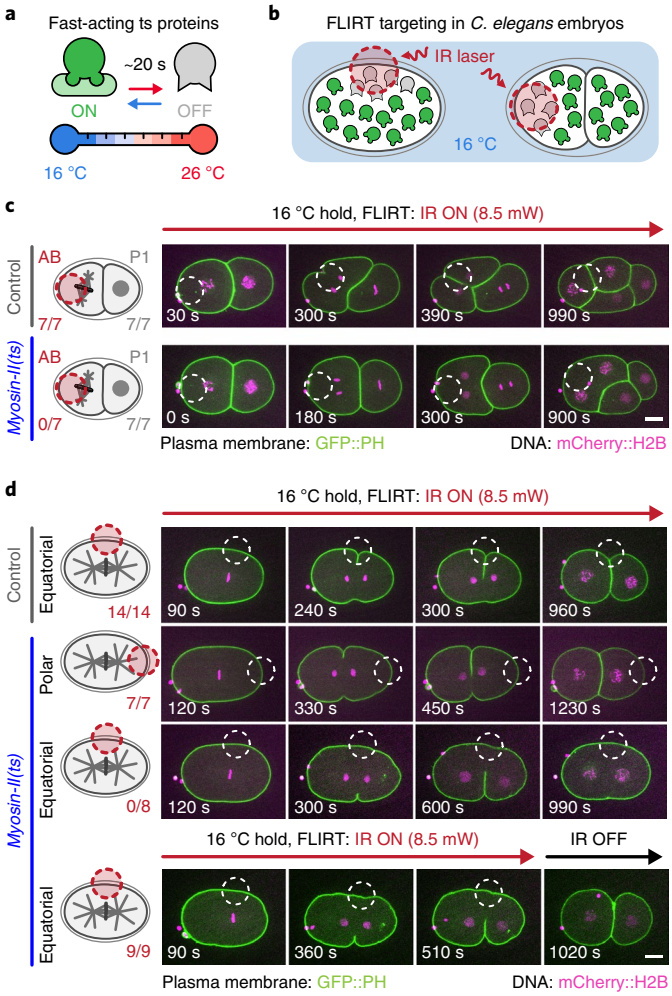

Fig. 1 | FLIRT calibration and application for spatiotemporal control of temperature-sensitive protein function in vivo. a, Fast-acting temperature-sensitive (ts) mutant proteins are rapidly inactivated on temperature upshift[3,6]. **b**, Schematic of FLIRT targeting in which an infrared laser is used to locally inactivate temperature-sensitive mutant protein function. **c**, Experimental schematic (left) and representative time-lapse images (right) of cell-specific FLIRT targeting in two-cell *C. elegans* embryos. See Supplementary Video 1. **d**, Experimental schematic (left) and representative time-lapse images (right) of subcellular FLIRT targeting either an equatorial or polar region in *myosin-II(ts)* one-cell embryos. Embryos were FLIRT-targeted either throughout division (top three rows; Supplementary Video 3) or for ~8 min to test reversibility (bottom row; Supplementary Video 5). The number of AB and P1 cells (**c**) or one-cell embryos (**d**) from biologically independent embryos that successfully completed cell division is indicated below each experimental schematic (left). Red (schematic) or white (images) dashed circles indicate the FLIRT-targeted regions. Time is in seconds after FLIRT initiation. Scale bars, 10 µm.

We next tested whether FLIRT can control temperature-sensitive mutant protein function with subcellular precision in the one-cell *C. elegans* embryo. During cytokinesis, myosin-II is enriched at the cell equator in the actomyosin contractile ring, where it is thought to drive ring constriction[10–12]. Myosin-II in the polar regions is not thought to drive ring constriction. Thus, we FLIRT-targeted (16-µm-diameter mask) either an equatorial or a polar region of dividing control and *myosin-II(ts)* embryos (Fig. 1d, Supplementary Fig. 5, and Supplementary Videos 3 and 4). Although FLIRT often caused a transient bleb in control embryos during equatorial targeting, probably as a result of local thermal gradients[13], it did not disrupt the normal polarity or asymmetry of this cell division (in contrast to other infrared systems[14]), embryo viability, or developmental timing (Supplementary Fig. 6), and all control embryos divided successfully (Fig. 1d and Supplementary Fig. 5a). In *myosin-II(ts)* embryos, FLIRT targeting one side of the equatorial region prevented contractile ring constriction on that side, but not on the non-targeted side. On the non-targeted side, the contractile ring initiated constriction but regressed on approaching the FLIRT-targeted region (Fig. 1d, Supplementary Fig. 5a, and Supplementary Videos 3 and 4). When we turned off the laser approximately 6 min after anaphase onset, both sides of the equator underwent ring constriction and cytokinesis was completed, again demonstrating that FLIRT inhibition of protein function is reversible (Fig. 1d, Supplementary Fig. 5a, and Supplementary Videos 5 and 6). Targeting the polar regions of *myosin-II(ts)* embryos or control embryos did not disrupt ring constriction (Fig. 1d and Supplementary Fig. 5a). Moreover, targeting the equatorial region in embryos expressing *Delta(ts)* (*apx-1(zu347ts)*[4]), a gene required for Delta–Notch cell fate signaling but not cytokinesis, did not disrupt cell division, thus demonstrating that the effects of FLIRT are specific to the temperature-sensitive mutant tested (Supplementary Fig. 5). These results suggest that FLIRT locally and reversibly inhibits temperature-sensitive mutant protein function with subcellular precision.

To confirm that FLIRT can disrupt temperature-sensitive mutant proteins with subcellular precision during a different cellular process, we used the *Delta(ts)* fast-acting temperature-sensitive allele[4] to perturb Delta–Notch-mediated cell fate signaling by targeting specific cell–cell contacts within the four-cell embryo. The four-cell *C. elegans* embryo consists of two anterior (ABa, ABp) and two posterior (EMS, P2) cells. Only the P2 cell expresses the transmembrane ligand Delta/APX-1 (hereafter Delta), while both the ABa and ABp cells express its transmembrane receptor, Notch/GLP-1 (hereafter Notch; Supplementary Fig. 7a)[4,15]. Direct cell–cell contact between P2 and ABp activates Notch in ABp, changing its cell fate and establishing dorsal–ventral embryonic polarity at the four-cell stage (Supplementary Fig. 7a)[4,5,16]. To monitor Delta–Notch signaling, we generated strains expressing a fluorescent Notch transcriptional reporter (*tbx-38p::mCherry::HistoneH1*[17–19]). This reporter is expressed in approximately 25% of the cells in late-stage embryos when Notch is activated in ABp, and in approximately 50% of cells when Notch activation in ABp is blocked (Fig. 2a and Supplementary Fig. 7b–e). We used FLIRT to target specific cell–cell contacts (16-µm-diameter mask) in control and *Delta(ts)* mutant embryos and monitored the effect on Delta–Notch signaling (Supplementary Fig. 7c). FLIRT targeting of the P2–ABp contact for approximately 25 min inhibited Delta–Notch signaling in *Delta(ts)* mutants, but not in control embryos, whereas FLIRT targeting of the P2–EMS contact had no effect (Fig. 2a), suggesting that FLIRT locally inhibits Delta–Notch cell fate signaling by targeting P2–ABp cell contacts.

Finally, we tested whether FLIRT can locally inhibit temperature-sensitive mutant protein function in the context of an adult worm tissue. Adult hermaphroditic *C. elegans* have a syncytial gonad in which germline nuclei undergo incomplete mitosis and are separated by membrane partitions but remain connected to the gonad via an intercellular bridge. The Rho-family GTPase activating protein CYK-4/MgcRacGAP (hereafter CYK-4) localizes to the intercellular bridges between germline membrane partitions and is required for oocyte production[20]. As was previously shown, upshift of *cyk-4(or749ts)* (hereafter *cyk-4(ts)*) adult worms to 26 °C led to a shortening of the membrane partitions that separate germline nuclei (Supplementary Fig. 8)[20]. FLIRT targeting (16-µm-diameter mask) of a single germline membrane partition in *cyk-4(ts)* worms led to a shortening of the FLIRT-targeted membrane partition but did not affect the length of membrane partitions between adjacent germline nuclei (Fig. 2b and Supplementary Video 7). FLIRT targeting of membrane partitions in control worms did not change partition length (Fig. 2b). Thus,

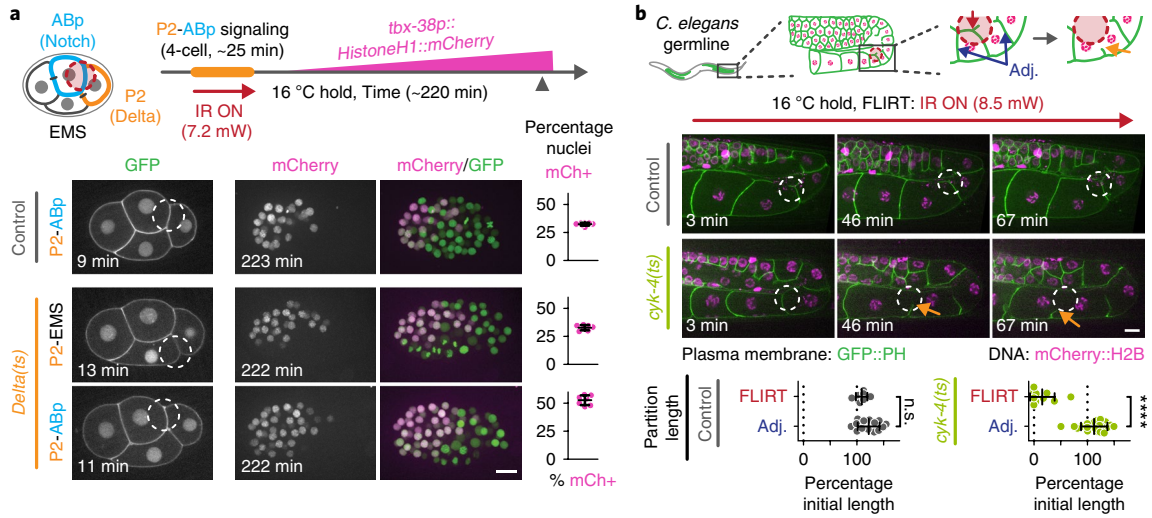

Fig. 2 | FLIRT for subcellular control of temperature-sensitive protein function. a, Experimental timeline schematic (top) and representative images (bottom) depicting FLIRT targeting either P2–ABp or P2–EMS cell–cell contacts in four-cell control and *Delta(ts)* embryos. Dot plots (right) show the percent total mCherry$^+$ (mCh+) nuclei at the ~50-cell stage (control P2–ABp $N=7$, *Delta(ts)* P2–EMS $N=7$, *Delta(ts)* P2–ABp $N=7$ biologically independent embryos). Green, GFP::PH (plasma membrane) and Histone(H2B/H3)::GFP (DNA); magenta, *tbx-38p::HistoneH1::mCherry* (Methods) **b**, Schematic (top) and representative time-lapse images (middle) depicting FLIRT targeting an individual membrane partition within the *cyk-4(ts)* adult *C. elegans* syncytial gonad. Arrows indicate membrane partition retraction. See Supplementary Video 7. Dot plots (bottom) showing the change in FLIRT-targeted and adjacent (Adj.) partition length after FLIRT targeting a single membrane partition in control and *cyk-4(ts)* worms shown as a percentage of initial length (control $N=7$, *cyk-4(ts)* $N=10$ biologically independent worms). Time elapsed is shown in minutes after FLIRT initiation. Red dashed circles (schematics) and white dashed circles (images) indicate the FLIRT-targeted ROIs. Unpaired two-tailed *t*-test; n.s., no significance, $P>0.05$; ****$P\leq0.0001$. Data are shown as mean ± s.d.; see Supplementary Table 1 for additional statistical analysis. Scale bars, 10 µm.

FLIRT can locally inhibit temperature-sensitive protein function with spatial resolution in germline tissue within the adult worm.

Together, our results demonstrate that FLIRT can locally inhibit protein function with cellular and subcellular precision. While we have applied this technology to studies of cell division, cell fate specification, and germline structure in *C. elegans*, we anticipate that FLIRT will be applicable to other cellular processes in model systems with available fast-acting temperature-sensitive mutants.

Online content

Any methods, additional references, Nature Research reporting summaries, source data, statements of data availability and associated accession codes are available at https://doi.org/10.1038/s41592-018-0168-y.

Received: 21 August 2017; Accepted: 10 August 2018;
Published online: 30 October 2018

References

1. Liu, J., Maduzia, L. L., Shirayama, M. & Mello, C. C. *Dev. Biol.* **339**, 366–373 (2010).
2. Severson, A. F., Hamill, D. R., Carter, J. C., Schumacher, J. & Bowerman, B. *Curr. Biol.* **10**, 1162–1171 (2000).
3. Davies, T. et al. *Dev. Cell.* **30**, 209–223 (2014).
4. Mickey, K. M., Mello, C. C., Montgomery, M. K., Fire, A. & Priess, J. R. *Development* **122**, 1791–1798 (1996).
5. Mello, C. C., Draper, B. W. & Priess, J. R. *Cell* **77**, 95–106 (1994).
6. Davies, T. et al. *Methods Cell Biol.* **137**, 283–306 (2017).
7. Kamei, Y. et al. *Nat. Methods* **6**, 79–81 (2009).
8. Sundaramoorthy, S. et al. *ACS Appl. Mater. Interfaces* **9**, 7929–7940 (2017).
9. Singhal, A. & Shaham, S. *Nat. Commun.* **8**, 14100 (2017).
10. D'Avino, P. P., Giansanti, M. G. & Petronczki, M. *Cold Spring Harb. Perspect. Biol.* **7**, a015834 (2015).
11. Pollard, T. D. *Curr. Opin. Cell Biol.* **22**, 50–56 (2010).
12. Green, R. A., Paluch, E. & Oegema, K. *Annu. Rev. Cell. Dev. Biol.* **28**, 29–58 (2012).
13. Oyama, K. et al. *Biophys. J.* **109**, 355–364 (2015).
14. Mittasch, M. et al. *Nat. Cell Biol.* **20**, 344–351 (2018).
15. Crittenden, S. L., Rudel, D., Binder, J., Evans, T. C. & Kimble, J. *Dev. Biol.* **181**, 36–46 (1997).
16. Shelton, C. A. & Bowerman, B. *Development* **122**, 2043–2050 (1996).
17. Murray, J. I. et al. *Genome Res.* **22**, 1282–1294 (2012).
18. Good, K. et al. *Development* **131**, 1967–1978 (2004).
19. Neves, A. & Priess, J. R. *Dev. Cell.* **8**, 867–879 (2005).
20. Lee, K. Y. et al. *eLife* **7**, e36919 (2018).

Acknowledgements

We thank all members of the Canman, Shirasu-Hiza, and Dumont laboratory for their support; H. Kim, I. Thomas, C. Walsh, B. Lesea-Pringle, K. Rimu, F. Jung, and E. Blake for laboratory assistance; C. Connors for comments on this manuscript; I. Greenwald, B. Bowerman, and B. Goldstein for helpful discussions; and J. Priess (Fred Hutchinson Cancer Research Center) and the *Caenorhabditis* Genomics Center for worm strains. We thank S. Wildfang, A. Ratz, and C. Anderson for technical assistance; A. Kummel and A. Garcia Badaracco for assistance on the thermochromatic dye analysis; and B. O'Shaughnessy, S. Wang, and S. Thiyagarajan for advice on thermal distribution. This work was funded by a Charles H. Revson Senior Fellowship in Biomedical Science (T.D.), FRM-DEQ20160334869 (J.D.); NIH-R01-GM105775 (S.M.H.); NIH-R01-AG045842 (MSH); NIH-DP2-OD008773 (J.C.C.); and NIH-R01GM117407 (J.C.C.).

Author contributions

S.M.H., S.S., T.D., and J.C.C. conceived of the experiments. S.M.H. and S.S. conducted all of the experiments with help from T.D. and Y.Z. J.C.W. and J.C.C. designed the microscope light path. S.M.H., S.S., T.D., M.S.H., J.C.W., J.D., and J.C.C. made intellectual contributions and wrote the manuscript. S.M.H., S.S., and J.C.C. made the figures.

Competing interests

The authors declare no competing interests.

Additional information

Supplementary information is available for this paper at https://doi.org/10.1038/s41592-018-0168-y.

Reprints and permissions information is available at www.nature.com/reprints.

Correspondence and requests for materials should be addressed to J.C.C.

Publisher's note: Springer Nature remains neutral with regard to jurisdictional claims in published maps and institutional affiliations.

Methods

The FLIRT microscope, imaging, and image analysis. The FLIRT microscope (Supplementary Fig. 1a) was built on a Ti inverted microscope stand (Nikon) equipped with a 60×/1.4-NA (numerical aperture) oil-immersion Plan Apo objective, a spinning disk confocal unit (CSU-10; Yokogawa) upgraded with Borealis (Spectral Applied Research), two 150-mW excitation lasers at 491 and 561 nm (Cairn), an emission filter wheel (Sutter Instruments) with two bandpass filters corresponding to 525/50 nm (Chroma no. ET525/50 m) and 620/50 nm (Chroma no. 620/60 m), and a cooled CCD (charge-coupled device) camera (Orca-R2; Hamamatsu Photonics). The system was controlled with MetaMorph software (Molecular Devices). A 3-W multimode 1,470-nm laser was used for FLIRT experiments (Rapp Optoelectronics GmbH). A mask wheel made of NBK-7 glass coated with aluminum (Rapp Optoelectronics GmbH) containing masks of distinct shapes and sizes was used to precisely target the infrared light on regions of interest (here a 16- or 27-µm-diameter mask was used) focused at the specimen plane. The infrared system, mask position, and laser power were controlled through Syscon Geo software (Rapp Optoelectronics GmbH). During all FLIRT experiments, focus was maintained relative to the coverslip using the CRISP auto focus system (Applied Scientific Instrumentation) before each image acquisition. Sunstone upconverting nanoparticles (also called Sunstone UCPs or nano^{545}-UCPs; Sigma-Aldrich no. 90992) mounted in H_2O between a slide and coverslip were used for infrared laser co-alignment with the visible light image path at the beginning of each experimental session as previously described[8].

All image analysis (including intensity measurements and line scan analysis) was performed using FIJI software[21] and graphs were generated in Prism 7 (GraphPad Software, Inc.) and imported into Adobe Illustrator CC (Adobe) to assemble the figures. Images were pseudo-colored and contrast adjusted for display using Adobe Photoshop CC.

Laser power measurements. The power of the 1,470-nm infrared laser was measured using an XLP12-3S-H2-DO detector and an accompanying Maestro power monitor (Gentec-EO), positioned near the imaging plane of the microscope. For each mask setting (16- or 27-µm diameter), the infrared laser power was varied and the mW values for each mask were monitored and averaged over a 2-min period from three independent measurements at each laser power setting.

Specimen temperature control and calibration. For all experiments, the specimens were mounted in a Peltier-controlled microfluidic specimen holder and temperature-control device (CherryTemp, Cherry Biotech) set to the indicated temperatures. Cherry software (Cherry Biotech) was used to control the temperatures of the heat exchangers and to designate the source for the flow chamber. To monitor the stability and accuracy of the set point temperature in the specimen holder, we mounted a microthermistor probe (Bioptechs no. 1917) with a drop of M9 buffer[22,23] (85 mM NaCl, 42 mM Na_2HPO_4, 22 mM KH_2PO_4, 1 mM $MgSO_4.7H_2O$), on the coverslip (No. 1.5, VWR no. 16004-312) with a round 2% agarose pad (Omnipur, CalbioChem) (~280 µm thick and 1 cm in diameter) placed between the probe and the microfluidic specimen holder to mirror the setup for FLIRT experiments with *C. elegans* embryos (see below). We measured the resistance at each set temperature at the coverslip with a multimeter (Mastech no. MS8220R) across a range of temperatures (8–30 °C), and we obtained an accurate estimation of temperature by using a temperature-versus-resistance conversion chart specific for the thermistor used. For FLIRT experiments, samples were mounted on a coverslip in M9 buffer (for all *C. elegans* experiments; Figs. 1 and 2 and Supplementary Figs. 3–7) or H_2O (for thermochromatic dye experiments; Supplementary Fig. 2), and a round 2% agarose pad (see above) was placed on top of the sample between the coverslip and the flow chamber of the microfluidic specimen holder.

Thermochromatic dye-based temperature measurement. Thermochromatic dyes that undergo a chromatic transition from opaque (black) to transparent at 15 °C (LCR Hallcrest LLC no. TS-COLDKIT) were mixed with a binder (LCR Hallcrest LLC no. TS-COLDKIT) and water in a 1:1:3 ratio, respectively. A thin film of the mixture was spread on a coverslip and allowed to air dry for approximately 30 min. Prior to imaging, approximately 5 µl of water was added onto the coverslip and a round 2% agarose pad was placed between the water drop and the specimen holder. To calibrate the change in transmitted light versus temperature, the whole thermochromatic-dye-coated coverslip was upshifted to specific temperatures at 0.5 °C or 1.0 °C increments across a thermal range from 8 to 20 °C, and images were collected at three different stage positions. For FLIRT calibration using the thermochromatic dye, either a 16- or a 27-µm-diameter mask was focused onto the dye at defined infrared laser powers (0–15 mW) while the background temperature was held at 9, 10, or 11 °C with the microfluidic specimen holder. Images were acquired every 60 s for temperature upshift experiments or every 30 s for FLIRT calibration with the thermochromatic dye, with 2×2 binning and 15×2.5 µm *z* sections. *z* sectioning was continually performed during the intervals between image acquisition, and the infrared laser was kept on for the duration of the experiment (to mirror FLIRT experiments with *C. elegans* embryos; see below). Mean intensity values within the FLIRT region of interest (ROI) were measured on the maximum intensity projected image at each laser power. For temperature upshift experiments, mean intensity values were measured inside an ROI of the same size as that used for the corresponding FLIRT experiments. Mean intensity values from the initial frame were subtracted and values were normalized to the maximum intensity for the whole sample temperature upshift experiment for each coverslip (Supplementary Fig. 2d,e). We determined the ratio of temperature to infrared laser power (mW per °C) by calculating the laser power required to reach the mean intensity values just before and just after the chromatic transition point (14, 14.5, 15, and 15.5 °C) from each of the holding temperatures (9, 10, or 11 °C) (Supplementary Fig. 2e).

mCherry::HistoneH2B biosensor-based temperature measurement. A *C. elegans* strain expressing mCherry::HistoneH2B (OD95)[24] was used as a temperature biosensor to calibrate the FLIRT microscope system. For these experiments, embryos at the approximately 100–200-cell stage were mounted in the microfluidic temperature-control device as described above. To plot a calibration curve, the temperature of the sample was varied across a thermal range between 16 and 26 °C and images were acquired at each temperature. For FLIRT experiments, embryos were held at 16 °C and subjected to FLIRT with defined laser powers (0–10 mW), and images were acquired every 30 s with an exposure time of 250 ms. For mCherry calibration experiments, images were acquired with a binning of 8×8 and 15×2.5 µm *z* sections. For all FLIRT experiments, *z* sectioning was continually performed between image acquisition. For image analysis, mean intensity values were measured on the sum projected raw image near the center of the FLIRT-targeted region of the embryo (4×4 µm^2 square). Two similar-sized ROIs were measured outside the embryo to determine the background intensity. We corrected the background-subtracted intensity values for bleaching by measuring the average rate of photobleaching for each replicate and then applying a bleach correction factor [(bleach rate) × (frame number) × (measured intensity)] for each frame to calculate its bleach-corrected intensity value. The intensity values for each frame were normalized to the average intensity value at 16 °C. We measured the relationship between mean intensity value and the change in temperature (ΔT) by monitoring the change in fluorescence intensity after defined temperature shifts and using linear regression modeling on these data in GraphPad Prism 7. Mean *y* values (relative fluorescence intensity) were considered for all *x* values (ΔT relative to 16 °C) between 0 and 10 °C, giving the relationship $y=-1.438x+99.61$, $R^2=0.99$ (Supplementary Fig. 3b, left panel). By performing similar image and linear regression analysis on embryos held at 16 °C and subjected to FLIRT with defined laser powers (3.84–9.75 mW), we measured a linear relationship between fluorescence intensity and laser power for both the 16-µm mask ($y=-1.641x+100$, $R^2=0.98$) and the 27-µm mask ($y=-1.595x+101$, $R^2=0.99$) (Supplementary Fig. 3b, right panel). Using linear regression analysis, we derived the relationship between ΔT (°C) and infrared laser power (mW) for the 16-µm mask ($y=1.088x$) and the 27-µm mask ($y=1.03x$).

H2B::mCherry biosensor-based thermal gradient measurement. For measurement of the thermal gradient induced by FLIRT, multicellular embryos (~100–200 cells) expressing mCherry::HistoneH2B (OD95) were mounted as described for biosensor temperature measurement. Specimens were held at a permissive temperature (16 °C in Supplementary Fig. 3d and Supplementary Fig. 7d, 10–16 °C in Supplementary Fig. 3e) and the ROI was targeted to one end of the embryo using either a 27-µm-diameter (Supplementary Fig. 3d) or 16-µm-diameter (Supplementary Figs. 3d,e and 7d) mask. Images were acquired with acquisition settings as described above for the mCherry::HistoneH2B biosensor-based temperature measurements, alternating between five frames acquired with the FLIRT laser off and five frames acquired with the FLIRT laser on with laser powers indicated for each experiment. For Supplementary Fig. 3d,e, the FLIRT laser was used to heat the region to approximately 25.5 °C with either the 27-µm mask (9.75 mW and 16 °C hold) or the 16-µm mask (8.5 mW and 16 °C hold; 10.1 mW and 14 °C hold; 12.3 mW and 12 °C hold; or 13.9 mW and 10 °C hold). For Supplementary Fig. 7d, the 16-µm mask was used to heat the region to approximately 24 °C (7.2 mW and 16 °C hold). For whole-embryo upshifts (Supplementary Fig. 3d), the same experimental setup was used and the temperature of the microfluidic temperature device was switched between 16 and 26 °C for five frames each.

For image analysis, FIJI[21] was used to generate a sum projection of all *z* sections and a 50-µm line scan across the entire embryo with a line thickness corresponding to the width of the FLIRT mask region (27 µm for Supplementary Fig. 3d, 16 µm for Supplementary Figs. 3d,e and 7d). A 50-µm-long line scan of the same thickness (27 or 16 µm) was used for background measurement, and line scans of the embryo were measured for the frames before and after the FLIRT laser was turned on or off (four measurements per embryo). The background measurement was averaged and subtracted from each value across the line scan, and the intensity values across the embryo for the frame with the laser turned on were normalized to the frames with the laser off (permissive temperature, 10–16 °C). A rolling average of five intensity values was calculated across the embryo. These intensity values were converted to calculated ΔT (°C) using the relationship between temperature and intensity found above ($y=-1.438x+99.61$), and the hold temperature was added to find calculated T (°C). Line scans displayed in Supplementary Figs. 3d,e and 7d only include *x* values between 2 and 45 µm to exclude the bright and variable signal from the extracellular polar bodies located at one end of the embryo.

Worm husbandry and embryo dissection. All worm strains used in this work were grown on normal growth media plates using standard *C. elegans* husbandry techniques[22,23] and maintained in incubators (Binder) set to 16 °C. Immediately prior to imaging, embryos of the appropriate stage were dissected from adult hermaphrodites into chilled M9 buffer (16 °C) and transferred onto the microfluidic specimen holder and temperature control device (16 °C) using a pulled needle mouth pipette for imaging as described[6].

The following worm strains were used in this study:

- *OD95: unc-119(ed3)* ltIs38[pAA1: pie-1p::GFP::PH(PLC1delta1); unc-119(+) III]; ltIs37 [pAA64; pie-1/mCHERRY::his-58; unc-119(+)]IV]*[25]
- *JCC637: nmy-2(ne3409ts)I; unc-119(ed3)* ltIs38[pAA1: pie-1p::GFP::PH(PLC1∂1); unc-119(+)III]; ltIs37[pAA64: pie-1p::mCHERRY::his-58; unc-119(+)]IV]*[1,3]
- *JCC744: unc-119(ed3)III; ddIs25[GFP::par-2;unc-119(+)]; ddIs26[mCherry::par-6;unc-119(+)]; unc-119(ed3)III*; ltIs37[pAA64; pie-1/mCHERRY::his-58; unc-119 (+)]IV*[26,27]
- *JCC596: unc-119(ed3)* ltIs38[pAA1: pie-1p::GFP::PH(PLC1delta1); unc-119(+)III]; zuIs178[his-72(1kb 5' UTR)::his-72::SRPVAT::GFP::his-72 (1KB 3' UTR)#+5.7 kb XbaI - HindIII unc-119(+)]; stIs10024[pie-1p::H2B::GFP; unc-119(+)]#; stIs10138[tbx-38p::HistoneH1-mCherry; unc-119(+)]*
- *JCC623: unc-119(ed3)* ltIs38[pAA1; pie-1p::GFP::PH(PLC1delta1); unc-119(+)III]; apx-1(zu347ts)V; zuIs178[his-72(1 kb 5' UTR)::his-72::SRPVAT::GFP::his-72 (1KB 3' UTR) #+5.7 kb XbaI - HindIII unc-119(+)]. stIs10024[pie-1p::H2B::GFP; unc-119(+)]#; stIs10138[tbx-38p::HistoneH1-mCherry; unc-119(+)]*[4]
- *OD239: unc-119(ed3)* cyk-4(or749ts) ltIs38[pAA1; pie-1::GFP::PH(PLC1delta1) unc-119 (+)]III; ltIs37[pAA64; pie-1::mCHERRY::his-58; unc-119 (+)]IV*[28]

For strains marked with an asterisk, the *unc-119(ed3)* mutation was present in the parental strains but has not been directly sequenced in these strains to determine whether the *unc-119* gene is mutated.

Strains annotated with a pound symbol (#) express Histone::GFP but have not been directly sequenced to determine which of the *his-72* and/or H2B transgenes are present; the GFP signal was used only as a marker for all nuclei.

Assaying cell division at permissive temperatures. For experiments to assess cell division defects at low background hold temperatures (Supplementary Fig. 3f), control one-cell embryos were dissected and mounted in the microfluidic specimen holder at a permissive temperature (between 10 and 16 °C) and maintained at that temperature throughout the experiment. Images were acquired from prometaphase through anaphase onset of the next cell division. Images were acquired every 30 s with 200-ms exposure for differential interference contrast (DIC) and 150-ms exposure times for the 491-nm and the 561-nm channels, with 2×2 binning and 15×2.5 µm *z* sectioning. Cell division outcomes were scored and divided into three phenotypic categories: (1) embryos in which cell division is completed without any visible defects, (2) embryos in which cytokinesis fails, or (3) embryos in which cell division is complete but which have minor defects during cell division. Minor division defects occur at low temperatures, probably owing to the inherent cold sensitivity of spindle microtubules[29], that lead to errors in mitotic spindle positioning, movement, and/or orientation.

FLIRT experiments targeting cell division in *myosin-II(ts)* and *Delta(ts)* mutants. For experiments to test the ability of FLIRT to locally inhibit myosin-II (NMY-2) activity with cellular (Fig. 1c and Supplementary Fig. 4) and subcellular (Fig. 1d and Supplementary Figs. 5a,b and 6b) precision, embryos from *C. elegans* strains OD95 (control), JCC637 (*myosin-II(ts)*), or JCC623 (*Delta(ts)*) were held at either 16 °C (Fig. 1c,d and Supplementary Figs. 4, 5b, and 6b) or 14 °C (Supplementary Figs. 5a and 6b) using the microfluidic specimen holder and subjected to FLIRT with the 16- or 27-µm-diameter masks. FLIRT experiments with the 27-µm mask were performed at approximately 6.1 mW (~22 °C) or at 9.8 mW (~26 °C) of infrared laser power (Supplementary Figs. 2 and 3, Supplementary Note 1). FLIRT experiments with the 16-µm mask (Fig. 1c,d and Supplementary Figs. 4, 5, and 6b) were performed with 8.5 mW (16 °C hold) or 10.1 mW (14 °C hold) of infrared laser power. FLIRT was turned on during prometaphase for all one-cell experiments (Fig. 1d and Supplementary Figs. 5 and 6b) and prometaphase of the AB cell for two-cell experiments (Fig. 1c and Supplementary Fig. 4) and was maintained on for the duration of the experiment through anaphase onset of the next cell division. During cytokinesis, the contractile ring in the AB cell mostly invaginates from the anterior of the cell and only slightly invaginates from the side of AB in direct cell contact with P1; thus in two-cell FLIRT experiments we targeted the division plane on the anterior side of the AB cell. Cytokinesis in P1 initiates from both sides of the cell, but to be consistent with the AB cell experiments, we targeted a posterior region of the P1 cell. For experiments to demonstrate the reversibility of FLIRT, embryos were subjected to an interval of FLIRT with the 16-µm mask for from prometaphase until 6 min after anaphase onset (Fig. 1d and Supplementary Fig. 5a) or 3–4 min after anaphase onset (Supplementary Fig. 4b). Images were acquired every 30 s with 200-ms exposure for DIC and 150-ms exposure times for the 491-nm and the 561-nm channels, with 2×2 binning and 15×2.5 µm *z* sectioning. *z* sectioning with the infrared laser was continually performed during the time interval between image acquisition. Completion or failure of cell division was assessed on anaphase onset of the next cell division.

Effect of FLIRT on anterior–posterior cell polarity. For experiments to test the effect of FLIRT on anterior–posterior cell polarity and daughter cell asymmetry during cell division (Supplementary Fig. 6a), *C. elegans* strain JCC744 (GFP::PAR-2; mCherry::PAR-6; mCherry::HistoneH2B) was held at either 16 °C or 14 °C in the microfluidic specimen holder. Embryos were monitored using DIC imaging until just prior to anaphase onset. Images were acquired every 3 min with 200-ms exposure for DIC, 150-ms exposure for the 491-nm channel, and 200-ms exposure for the 561-nm channel, with 2×2 binning and 15×2.5 µm *z* sectioning. Experiments were either done with no FLIRT (0 mW) or with the 16-µm mask targeting the equatorial region with either 8.5 mW of laser (16 °C hold temperature) or 10.1 mW (14 °C hold temperature). When infrared was used, FLIRT was initiated prior to anaphase onset and *z* sectioning with the infrared laser was continually performed during the time interval between image acquisition to maintain local control of temperature. For analysis of cell polarity and daughter cell asymmetry[30], measurement of the size of the AB and P1 cells were performed in FIJI[21]. The GFP and mCherry signals were measured separately to determine cell size both during cell division and at the two-cell stag; cell polarity and daughter cell asymmetry were measured[30] as the difference between AB and P1 size in micrometers.

Post-FLIRT embryo viability analysis. Following an individual FLIRT experiment targeting the equatorial region of a dividing control embryo (16-µm mask; held at either 16 °C with 8.5 mW or 14 °C with 10.1 mW; see the section "FLIRT experiments targeting cell division in *myosin-II(ts)* and *Delta(ts)* mutants" above for details) at the one-cell stage, the microfluidic temperature device was removed and the 2% agar pad containing the embryo was lifted from its bottom surface with a scalpel. The agar pad was then placed embryo-side down onto normal-growth-media worm plates (see also the section "Worm husbandry and embryo dissection" above) containing OP50 bacteria and maintained at 16 °C to allow embryo development and hatching. For non-FLIRT controls, one-cell-stage embryos were dissected in M9 buffer (see above) and individually placed onto a separate normal-growth-media plate using a pulled needle mouth pipette and maintained at 16 °C. Images of the FLIRT and non-FLIRT control isolated embryos were acquired every 16–24 h from hatching and into adulthood with a Micropublisher 3.3 RTV camera (Q-Imaging) mounted on the C-mount of a dissecting microscope (Olympus SZX16) with a 120-ms exposure time using QCapture Suite Plus software (Q-Imaging) to ensure development was timely and adult reproduction was not grossly affected. Viability was measured as the percentage of embryos that hatched within 24 h of dissection.

Delta–Notch activity reporter characterization and FLIRT assay. Late two-cell-stage embryos were dissected from control (JCC596) and *Delta(ts)*[4,5] (JCC623) adult worms and mounted in the imaging chamber of the temperature-control device (16 °C). For whole-cell upshift experiments (Supplementary Fig. 7e), embryos were either held at 16 °C or upshifted to 22, 24, or 26 °C for the duration of the experiment. For the four-cell brief time window temperature upshift experiments, embryos were mounted at 16 °C at the late two-cell stage. The temperature was increased to 24 or 26 °C at the early four-cell stage, then shifted back down to 16 °C following anaphase onset of the P2 cell and maintained at 16 °C for the duration of the experiment. For whole-cell upshift experiments (Supplementary Fig. 7e), images in the 491- and 561-nm channels were acquired every 20 min for 3 h, from the late two-cell stage through the approximately 200-cell stage. For FLIRT experiments (Fig. 2a), the embryos were maintained at 16 °C. Images were acquired as described above with 200-ms exposure for DIC, 150-ms exposure time for the 491-nm channel, and 250 ms for the 561-nm channel with 2×2 binning and 15×2.5 µm *z* sectioning for all experiments. Following the initial time point at late anaphase of the P1 cell, the P2 cell was targeted with 7.2 mW of infrared laser power (16-µm mask) at the cell–cell contact between P2 and the ABp cell (control and *Delta(ts)*) or the EMS cell (*Delta(ts)*). The infrared laser remained on and images were acquired every 60 s with continuous 15×2.5 µm *z* sectioning between image acquisition through anaphase onset of the P2 cell (~20 min), when the infrared laser was turned off. After the infrared laser was turned off, embryos were maintained at 16 °C and images were acquired every 20 min for another 3 h until the approximately 200-cell stage.

For ABp cell fate experiments, image analysis was done in FIJI[21] using the Cell Counter plugin (https://imagej.nih.gov/ij/plugins/cell-counter.html). At the approximately 50-cell stage (160 min post-FLIRT), Cell Counter was used to manually identify the total number of GFP^+ and $mCherry^+$ nuclei. We determined the percentage of Notch-activated cells by quantifying the percentage of all GFP^+ nuclei that were also $mCherry^+$. The percentage of $GFP^+mCherry^+$ nuclei was quantified for control and *Delta(ts)* embryos from whole-cell upshifts and FLIRT experiments (for statistical analysis see also Supplementary Table 1).

FLIRT experiments with *cyk-4(ts)*. Control (OD95) and *cyk-4(ts)* (OD239) early adult worms were picked into 5 µl of M9 buffer and 0.25–0.5 µl of 0.1-µm-diameter polystyrene microspheres (Polysciences 00876-15, 2.5%

w/v suspension) then covered with a pad made of 10% agarose in M9 for immobilization[31] and mounted in the microfluidic specimen holder set to 16 °C. For upshift experiments (Supplementary Fig. 8), the temperature-control device was shifted to 26 °C approximately 5 min after mounting. Images of the gonad were acquired every 60 s for 75 min with 200-ms exposure for DIC and 150-ms exposure times for the 491-nm and the 561-nm channels, with 2 × 2 binning and 15 × 2.5 µm *z* sectioning. For FLIRT experiments (Fig. 2b), the 16-µm mask (8.5 mW) was positioned to target a single membrane partition on the proximal side of the gonad after the bend of the gonad arm and moved to follow the same membrane partition within the worm. Images were acquired every 60 s and *z* sectioning with the infrared laser was continually performed during the time interval between image acquisition.

We analyzed compartment partition length in FIJI[21] by measuring the length of individual compartment partitions on the frame just after FLIRT was turned on and 70 min after upshift or FLIRT targeting. Membrane partition length was measured from the site of contact with the edge of the gonad to the end of the membrane partition at the central germline rachis using a segmented line on the *z* section in which the partition was longest. The percentage initial length was measured as a percentage of membrane partition length at $t = 70$ min divided by the length at $t = 0$ min. For upshift experiments (Supplementary Fig. 8), four individual compartment partitions were analyzed for each worm. For FLIRT experiments (Fig. 2b), the FLIRT-targeted partition and the two adjacent non-targeted partitions were analyzed.

Statistical analysis. Unpaired two-tailed Student's *t*-tests were conducted using Microsoft Excel. Not significant, $P \geq 0.05$; $^{*}P < 0.05$, $^{**}P < 0.01$, $^{***}P < 0.001$, and $^{****}P < 0.0001$. In Supplementary Fig. 7e, Tukey's test for multiple comparisons was conducted using GraphPad Prism software, $\alpha = 0.05$. Error bars represent the s.d. except in Supplementary Fig. 2d,e and the gradient analysis in Supplementary Figs. 3d,e and 7d, where error bars represent the s.e.m. See also Supplementary Table 1 and the Nature Research Reporting Summary.

Reporting Summary. Further information on research design is available in the Nature Research Reporting Summary linked to this article.

Data availability

The data that support the findings of this study are available from the corresponding author upon reasonable request.

References

21. Schindelin, J. et al. *Nat. Methods* **9**, 676–682 (2012).
22. Brenner, S. *Genetics* **77**, 71–94 (1974).
23. Stiernagle, T. Maintenance of *C. elegans*. *WormBook* https://doi.org/10.1895/wormbook.1.101.1 (2006).
24. Audhya, A. et al. *J. Cell Biol.* **171**, 267–279 (2005).
25. Ai, E., Poole, D. S. & Skop, A. R. *Mol. Biol. Cell* **20**, 1629–1638 (2009).
26. Jordan, S. N. et al. *J. Cell Biol.* **212**, 39–49 (2016).
27. Schonegg, S., Constantinescu, A. T., Hoege, C. & Hyman, A. A. *Proc. Natl Acad. Sci. USA* **104**, 14976–14981 (2007).
28. Canman, J. C. et al. *Science* **322**, 1543–1546 (2008).
29. Widlund, P. O. et al. *Mol. Biol. Cell* **23**, 4393–4401 (2012).
30. Bossinger, O. & Cowan, C. R. *Methods Cell Biol.* **107**, 207–238 (2012).
31. Kim, E., Sun, L., Gabel, C. V. & Fang-Yen, C. *PLoS One* **8**, e53419 (2013).

nature research

Corresponding author(s): Julie C. Canman

☐ Initial submission ☒ Revised version ☐ Final submission

Life Sciences Reporting Summary

Nature Research wishes to improve the reproducibility of the work that we publish. This form is intended for publication with all accepted life science papers and provides structure for consistency and transparency in reporting. Every life science submission will use this form; some list items might not apply to an individual manuscript, but all fields must be completed for clarity.

For further information on the points included in this form, see Reporting Life Sciences Research. For further information on Nature Research policies, including our data availability policy, see Authors & Referees and the Editorial Policy Checklist.

Experimental design

1. Sample size

Describe how sample size was determined.

The high reproducibility of events in C. elegans does not require a particularly high number of individual embryos to be analyzed. For each experiment presented in this study, the sample size is equal or higher to sample size observed in most published studies. Since worms are treated individually and a different worm is used to obtain each embryo, each embryo is be considered as an individual experiment.

2. Data exclusions

Describe any data exclusions.

No data were excluded.

3. Replication

Describe whether the experimental findings were reliably reproduced.

For each experiment involving C. elegans embryos or adult worms, at least 6 (and up to 20) individual embryos were analyzed, isolated from the same number of individual adult hermaphrodites; and all experiments for temperature calibration of the FLIRT system were done in replicates of 4 (thermochromatic dye) or 7 (mCherry fluorescence) to ensure reliability and reproducibility. All attempts at replication were successful.

4. Randomization

Describe how samples/organisms/participants were allocated into experimental groups.

Experimental groups were allocated based upon genotype. In experiments with multiple experimental conditions per genotype, embryos were randomly selected for each experimental condition. Both control and ts mutant genotypes were used within a given day of FLIRT experimentation.

5. Blinding

Describe whether the investigators were blinded to group allocation during data collection and/or analysis.

The investigators were not blinded to allocation during experiments and outcome assessment due to the nature of the microscopy experiments and the necessity to keep track of the genotype, time of temperature upshift, and the time of IR laser irradiation for each individual time lapse image series, as is consistent within the field.

Note: all studies involving animals and/or human research participants must disclose whether blinding and randomization were used.

6. Statistical parameters

For all figures and tables that use statistical methods, confirm that the following items are present in relevant figure legends (or in the Methods section if additional space is needed).

n/a	Confirmed
☐	☒ The exact sample size (*n*) for each experimental group/condition, given as a discrete number and unit of measurement (animals, litters, cultures, etc.)
☐	☒ A description of how samples were collected, noting whether measurements were taken from distinct samples or whether the same sample was measured repeatedly
☐	☒ A statement indicating how many times each experiment was replicated
☐	☒ The statistical test(s) used and whether they are one- or two-sided (note: only common tests should be described solely by name; more complex techniques should be described in the Methods section)
☐	☒ A description of any assumptions or corrections, such as an adjustment for multiple comparisons
☐	☒ The test results (e.g. *P* values) given as exact values whenever possible and with confidence intervals noted
☐	☒ A clear description of statistics including central tendency (e.g. median, mean) and variation (e.g. standard deviation, interquartile range)
☐	☒ Clearly defined error bars

See the web collection on statistics for biologists for further resources and guidance.

Software

Policy information about availability of computer code

7. Software

Describe the software used to analyze the data in this study.	ImageJ (FIJI), Graphpad Prism, and Microsoft Excel were used for all data analysis.

For manuscripts utilizing custom algorithms or software that are central to the paper but not yet described in the published literature, software must be made available to editors and reviewers upon request. We strongly encourage code deposition in a community repository (e.g. GitHub). *Nature Methods* guidance for providing algorithms and software for publication provides further information on this topic.

Materials and reagents

Policy information about availability of materials

8. Materials availability

Indicate whether there are restrictions on availability of unique materials or if these materials are only available for distribution by a for-profit company.	After publication, all worm strains used in this study will be made available to researchers upon request.

9. Antibodies

Describe the antibodies used and how they were validated for use in the system under study (i.e. assay and species).	No antibodies were used in this study.

10. Eukaryotic cell lines

a. State the source of each eukaryotic cell line used.	No cell lines were used in this study.
b. Describe the method of cell line authentication used.	No cell lines were used in this study.
c. Report whether the cell lines were tested for mycoplasma contamination.	No cell lines were used in this study.
d. If any of the cell lines used are listed in the database of commonly misidentified cell lines maintained by ICLAC, provide a scientific rationale for their use.	No cell lines were used in this study.

Animals and human research participants

Policy information about studies involving animals; when reporting animal research, follow the ARRIVE guidelines

11. Description of research animals

Provide details on animals and/or animal-derived materials used in the study.	This study involved the use of the invertebrate C. elegans. No vertebrate animals were used in this study.

Policy information about studies involving human research participants

12. Description of human research participants

Describe the covariate-relevant population characteristics of the human research participants.	No human subjects were used in this study.